

Y-Trim: Evidence-gated per-read trimming for stochastic end artifacts in ssWGBS

Yihan Fang^{1,*}

¹School of Engineering, Tufts University, 177 College Ave, 02155, Medford, USA

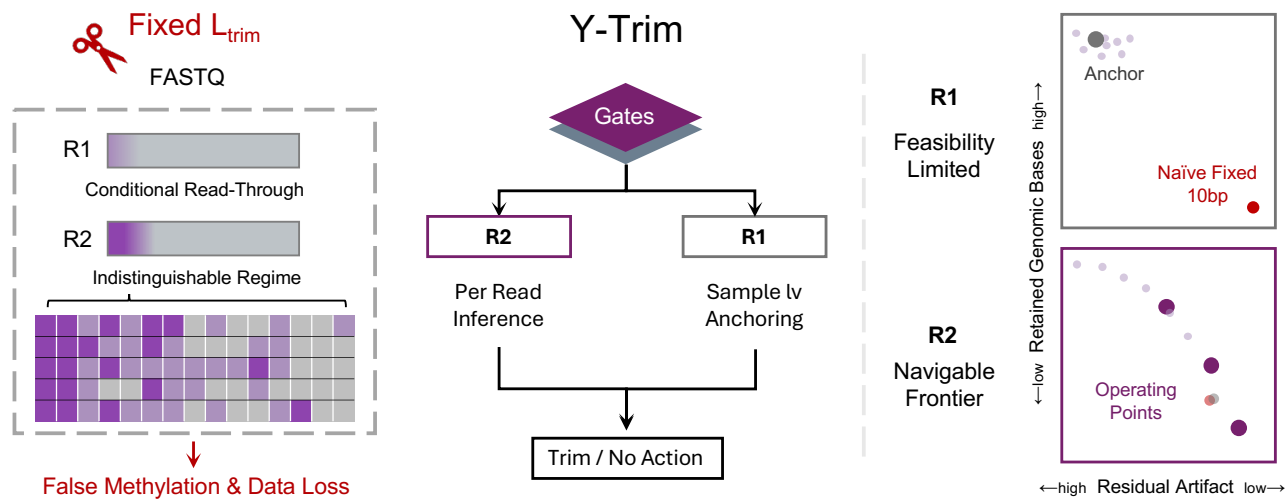
*Corresponding author. yihan.fang@tufts.edu

Abstract

Single-stranded whole-genome bisulfite sequencing (ssWGBS) profiles DNA methylation in low-input and fragmented samples, yet Adaptase-mediated tailing creates stochastic artifacts that obscure true genomic ends. Current deterministic trimming methods struggle because, as we show, bisulfite-induced degeneracy creates a locally indistinguishable regime with a strictly positive Bayes error, making exact per-read boundary recovery ill-posed from FASTQ observables alone. As a result, fixed trimming rules inevitably mix over-trimming (avoidable genomic loss) and under-trimming (residual artifactual signal) under heterogeneous tail-length regimes, amplifying end-proximal bias in methylation-relevant summaries. Here we present Y-Trim, an evidence-gated trimming framework that operationalizes these constraints. Y-Trim separates admission from inference: sample-level gating activates trimming only when chemistry-consistent evidence is present, and read-level logic treats Read 2 and Read 1 asymmetrically, reflecting kinetic tailing versus conditional read-through geometry. With explicit safeguards—including abstention under non-separable evidence—Y-Trim bounds action without forcing false precision. Using a chemistry-consistent simulator with ground truth and a 34-sample public cohort (CCGB-34), we show that Y-Trim yields an interpretable retention-risk frontier on Read 2 while revealing feasibility-limited behavior on Read 1, and achieves competitive end-proximal artifact suppression relative to common fixed-length practice. Y-Trim provides a practical, uncertainty-aware preprocessing step for high-precision ssWGBS methylation studies.

Keywords DNA methylation, single-stranded whole-genome bisulfite sequencing (ssWGBS), sequencing artifacts, read trimming, boundary inference, Adaptase, quality control

Graphical Abstract



Key Messages

- **The Problem:** Adaptase tailing creates stochastic artifacts that confound standard trimming and introduce methylation bias.
- **The Insight:** We establish an intrinsic identifiability limit: deterministic boundary inference incurs strictly positive Bayes error.
- **The Solution:** Y-Trim employs evidence-gated safeguards to recover maximal information strictly within these theoretical bounds.

Introduction

ssWGBS and post-bisulfite end artifacts

Single-stranded whole-genome bisulfite sequencing (ssWGBS) extends genome-wide DNA methylation profiling to sample types where conventional double-stranded workflows often fail, including low-input, highly fragmented, and cell-free DNA material.[19, 17, 18] These advantages come with distinctive preprocessing challenges that arise from post-bisulfite library construction. In widely used chemistries, Adaptase-mediated tailing introduces synthetic, template-free end sequence whose length and composition are stochastic and chemistry-dependent.[3, 4, 1, 2] Unlike ligated adapters, which are deterministic and can be removed by standard adapter-trimming logic, Adaptase-driven end artifacts do not have a fixed cut-point. As a result, the boundary between genomic sequence and synthetic end artifacts can be blurred, and trimming becomes a persistent source of variability across analytical pipelines.

A key complication is that this artifact is *structurally asymmetric* between paired-end reads. By sequencing geometry, Read 2 typically initiates within the Adaptase-tailed region, so synthetic sequence is systematic and boundary handling is unavoidable. In contrast, Read 1 contains synthetic sequence only conditionally under read-through when read length exceeds insert length, making contamination sparse and geometry-driven rather than ubiquitous. This asymmetry implies that a single uniform trimming rule is unlikely to be well-matched to both reads. In particular, Read2 initiates systematically within the Adaptase-tailed region, whereas Read1 contamination is conditional on insert-length read-through (Fig. 1A).

FASTQ-level observability and the trimming problem

Despite its practical importance, trimming in ssWGBS is often implemented in practice as a fixed, sample-level truncation applied uniformly across reads.[12, 13] Such constant trimming is attractive as a robust engineering fallback: it is simple, fast, and avoids overfitting to noisy per-read patterns. However, it also sidesteps the central inferential question: *what can be inferred about the artifact–genome boundary from FASTQ-level observables alone?* This is not a purely algorithmic issue. Bisulfite conversion collapses sequence complexity, and the synthetic artifact and genomic sequence share the same nucleotide alphabet in the observed reads. Consequently, local sequence evidence can enter an intrinsically indistinguishable regime where “artifact-like” and “genome-like” fragments share support under the same observable features, implying a strictly positive error floor for any deterministic per-read boundary rule (formalized in Supplementary Note 1). In this regime, per-read trimming cannot be made “correct” by better heuristics alone; instead, trimming must be structured as a constrained decision problem that acts only where evidence is admissible and remains conservative where it is not.

These observability limits interact with the paired-end asymmetry above. For Read 2, Adaptase-driven signatures can exhibit kinetically structured local statistics (short-range nucleotide texture) that support *constrained* read-level inference within an admissible transition regime. For Read 1, apparent contamination arises conditionally from read-through geometry and is not well-defined at the single-read level in the same way, making per-read action far harder to justify. Together, these considerations motivate an approach that (i) separates *admission control* (whether trimming is

warranted) from (ii) *read-level inference* (where evidence supports it), and (iii) permits explicit non-action (abstention) as a first-class outcome when evidence is insufficient.

Contributions and overview

Here we formalize ssWGBS trimming as a FASTQ-level inference problem under constrained observability and introduce a conservative framework that makes these constraints operational. Our main contributions are:

- **Observability limits and asymmetry.** We characterize why per-read boundary inference is intrinsically limited in post-bisulfite ssWGBS, including an indistinguishable regime that implies a non-zero Bayes error floor, and we show that boundary inference is fundamentally asymmetric between Read 2 (systematic artifacts; constrained inference feasible) and Read 1 (conditional, geometry-driven read-through; read-level inference often ill-defined).
- **Evidence-gated decision framework.** We introduce **Y-Trim**, an evidence-gated trimming framework with explicit safeguards—including abstention—that operates only where observable sequence texture supports inference, treats paired-end reads asymmetrically, and avoids forced resolution in intrinsically unsupported regimes.
- **Ground-truth stress testing and real-data evaluation.** Because per-read ground truth is not observable in real ssWGBS, we develop a chemistry-consistent generative simulator to enable controlled stress tests with known boundaries, and we evaluate Y-Trim on a curated real-data collection (CCGB-34) to map interpretable retention–risk behavior and demonstrate improved uncertainty-aware preprocessing outcomes.

The remainder of the manuscript is organized as follows. We first detail materials, datasets, and the simulator and decision framework (Materials and Methods). We then present results in three parts: (i) empirical and statistical constraints that bound per-read inference, (ii) Y-Trim’s decision logic and behavior under controlled uncertainty, and (iii) real-data trade-offs and downstream implications for methylation-relevant summaries. Finally, we discuss how the evidence-gated framing generalizes to other stochastic, texture-defined sequencing end artifacts beyond ssWGBS.

Materials and Methods

FASTQ-level observables and pipeline position

Y-Trim is a pre-alignment preprocessing step for post-bisulfite ssWGBS libraries. At this stage, the only universally available and consistently interpretable signal is the base-call string in each FASTQ record (A/C/G/T/N) together with positional order. Accordingly, Y-Trim restricts inference to sequence identity and local sequence statistics computed directly from the FASTQ stream, and does not assume access to alignment, reference consistency, read merging/overlap reconstruction, or other downstream signals.

Base quality scores are intentionally excluded from decision-making. Our design goal is a chemistry-typed rule that is portable across platforms and does not depend on run-specific calibration of quality encodings or platform-specific error models. Moreover, under bisulfite-induced compositional collapse, base identity (including N) is the only FASTQ-level signal that remains directly comparable

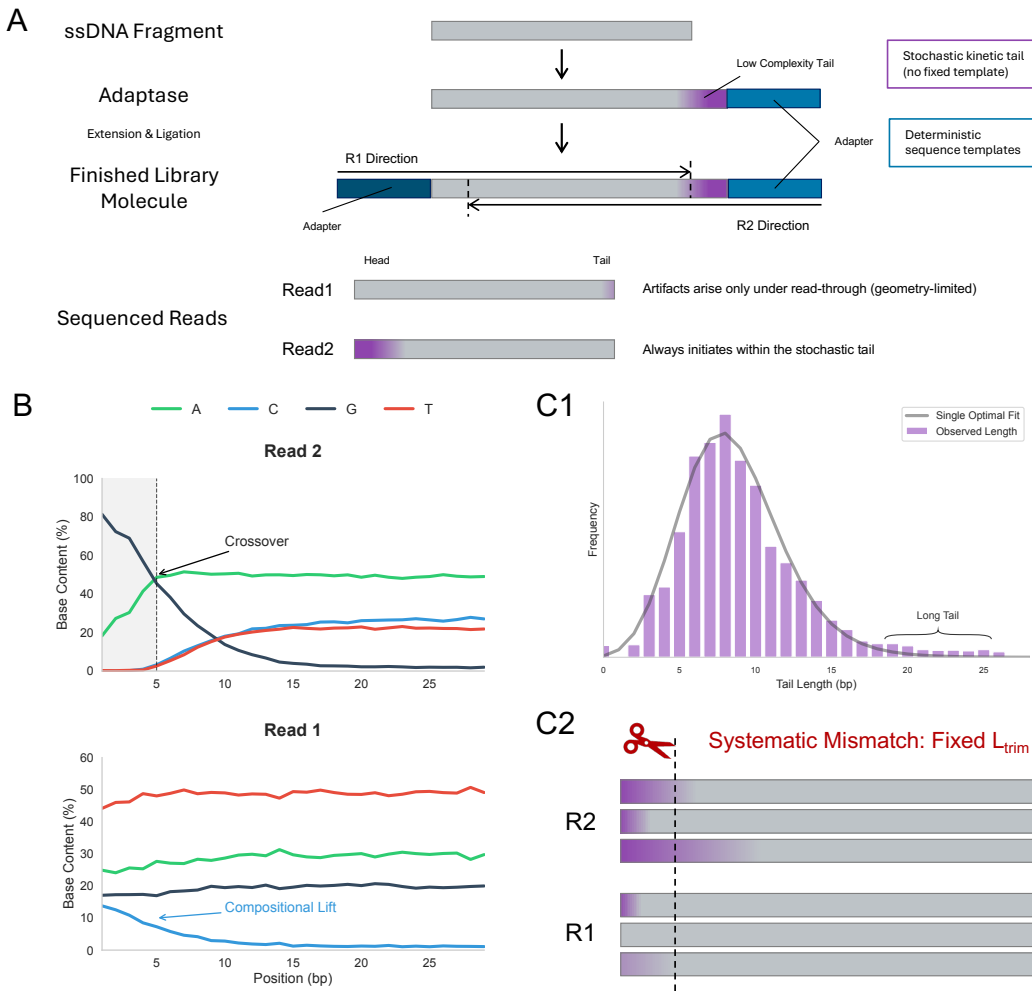


Figure 1 Why ssWGBS trimming is an evidence-limited, asymmetric FASTQ-stage decision. (A) Physical origin of post-bisulfite end artifacts and paired-end asymmetry: Read 2 initiates systematically within the Adaptase-tailed region, whereas Read 1 contamination arises only conditionally under insert-length read-through. (B) FASTQ-level observability: local nucleotide texture provides chemistry-consistent evidence but contains an intrinsically indistinguishable transition regime in which genomic and synthetic origins share support. (C1) Read 2 exhibits pronounced tail-length heterogeneity with a heavy long tail, consistent with systematic Adaptase-driven contamination and frequent extended or mixed regimes beyond a single typical boundary scale. Read 1 is not shown in (C1) because contamination arises conditionally from insert-length read-through and does not yield an analogous per-read tail-length structure at the FASTQ stage. (C2) Consequence of fixed-length trimming: any global cut inevitably mixes over-trimming (loss of genomic bases in short-tail reads) and under-trimming (residual artifacts in long-tail reads).

without introducing additional assumptions. Accordingly, ambiguity is handled explicitly through nucleotide content (including N), while coarse quality screening remains the responsibility of upstream FASTQ hygiene (e.g., adapter removal and gross filtering).

Operationally, Y-Trim treats read pairs asymmetrically based on the physical origins of end artifacts in post-bisulfite libraries. The method acts on reads independently and does not require read merging; paired-end structure enters only through the chemistry- and geometry-driven feasibility differences between Read 2 and Read 1 described below.

Stable observables, identifiability limits, and asymmetric feasibility

Sample-level PBSC as a diagnostic, not an optimization target

Per-base sequence content (PBSC)—the position-wise base-frequency profile aggregated across reads—is a stable sample-level observable

in ssWGBS and provides a chemistry-consistent summary of early-cycle end behavior at the population level (Figure 1B; Supplementary Note 2). PBSC is computable directly from FASTQ prior to alignment and is commonly reported by standard QC tooling.

PBSC plays two roles in this work. First, it provides a *sample-level admission signal*: PBSC patterns in a short prefix window are used to decide whether chemistry-consistent end-artifact evidence is present and whether downstream read-level inference is admissible (Supplementary Note 2). Second, composition-based summaries computed from FASTQ base composition (PBSC) are used for reporting to contextualize the direction of trimming outcomes (e.g., whether residual artifact-like composition remains near the read start), but they are not treated as a primary objective to be optimized (Figure 3; Supplementary Note 8).

Importantly, we do not define trimming as “matching” a universal PBSC target profile. PBSC is shaped jointly by biological base

composition, chemistry-specific artifact statistics, and insert-length geometry; therefore, a visually “clean” PBSC profile does not imply that per-read boundaries were correctly resolved, nor does it uniquely determine a correct cut position. Because trimming is an irreversible per-read intervention, explicitly optimizing a PBSC-like population summary can reduce apparent end bias by deleting genome-derived sequence along with artifact-like sequence. For this reason, PBSC is used as an admissibility diagnostic and a reporting coordinate, while per-read cuts are chosen by the evidence-gated inference rule rather than by PBSC matching.

Read-level evidence via short-range texture and an irreducible error floor

At the read level, ssWGBS end artifacts are template-free additions produced by a stochastic kinetic process, while bisulfite conversion reduces effective sequence complexity. This combination yields regimes where chemistry-specific compositional contrast is present (notably dominant-G signatures in Read 2 for Adaptase-based workflows), but perfect boundary localization is not achievable from sequence alone. Empirically, the transition is heterogeneous across reads and positions, with local mixing that is visible in the base-level visualization (Figure 2, top left).

We treat short-range *texture* as the most informative *local* cue available at the FASTQ stage: low-order statistics of the observed sequence (e.g., 2-mers/short k-mers and their position-dependent transitions) that capture chemistry-typed kinetic structure without assuming a fixed artifact template. Texture is emphasized because the artifact is not defined by a deterministic motif but by reproducible local statistics induced by chemistry and kinetics. In Y-Trim, these local cues are combined with cumulative, position-indexed evidence across a fixed prefix horizon, so the decision is based on aggregated FASTQ-level information rather than any single local feature (Section 2.6.2).

Even when texture cues are combined with all other FASTQ-level information within our scope (base identities, positional order, and their cumulative structure), bisulfite-induced compositional overlap creates an intrinsically indistinguishable regime in which genomic and synthetic origins assign non-zero probability to the same observable configurations under the same nucleotide alphabet. In this overlap regime, any deterministic per-read boundary rule has a strictly positive Bayes error (formalized in Supplementary Note 1). Therefore, read-level boundary inference is treated as constrained decision-making: contract the boundary to an admissible transition regime when cumulative evidence is separating, and avoid forced point localization when evidence remains non-separating.

Paired-end asymmetry and feasibility: Read 2 is systematic; Read 1 is conditional

Post-bisulfite library construction and sequencing geometry induce a structural asymmetry between paired-end reads (Figure 1A). Read 2 necessarily initiates within the enzymatic tail region in Adaptase-based designs, so synthetic signal is systematic and boundary handling is routinely required. Read 1, in contrast, contains synthetic sequence only under read-through when read length exceeds insert length; apparent contamination is therefore conditional on fragment geometry and is statistically independent of the tailing process itself.

This has two operational consequences. First, Read 2 often admits meaningful read-level inference (within the identifiability limits above), because artifact signal is present in the majority of

reads and chemistry-specific contrast is often strong; a representative example illustrating the prevalence of Read 2 tail-derived signal is shown in Figure 1C1. Second, Read 1 is not “a weaker Read 2”: its contamination arises from a superposition of a geometry-driven read-through condition and stochastic tailing, and is frequently not well-posed at single-read resolution. Accordingly, Read 1 is treated as a feasibility-limited setting where conservative sample-level anchoring and abstention are appropriate default behaviors (Supplementary Notes 2 and 5); this separation also motivates why naively applying Read 2-style per-read logic as if Read 1 were simply a weaker instance can lead to systematic mismatch between intervention and evidence (Figure 1C2).

Reporting directions: avoidable genomic loss versus residual artifact carryover

Because per-read ground-truth boundaries are unobservable in real ssWGBS data, evaluation should not rely on scalar “read retention” as a universal objective: retained bases may reflect either preserved genomic sequence or preserved synthetic contamination. Instead, we report trimming behavior along two chemistry-consistent directions corresponding to the two structural error modes of any boundary decision: (i) avoidable genome-like loss due to over-trimming (cutting past the transition), and (ii) residual artifact-like carryover due to under-trimming (cutting before the transition). These directions are instantiated as two fixed, FASTQ-stage reporting axes (Axis 1 and Axis 2) defined in Supplementary Note 8.2.3 and Supplementary Note 8.2.4, and are used to construct the Read 2 operating-point frontier and to summarize the feasibility-limited Read 1 behavior shown in Fig. 3 A1–A2.

Datasets and controlled evaluation design

CCGB-34 real-data surface.

We assembled CCGB-34 (Comprehensive Cell-free & Genomic Bisulfite; $n = 34$) as a scenario-indexed ssWGBS evaluation surface spanning diverse sample contexts (including cfDNA, low-input tissue/LCM, and FFPE) and protocol variants. CCGB-34 is not treated as a read-level “ground-truth” benchmark; rather, it is curated to expose operational regimes that matter for trimming decisions, including (i) canonical Adaptase tailing in Read 2, (ii) geometry-limited feasibility for Read 1 via conditional read-through, (iii) benign early-position fluctuations that can resemble contamination at the PBSC level, and (iv) negative-control/non-Adaptase libraries where trimming should abstain. Scenario definitions, accession manifests, and reporting axes are provided in Supplementary Note 8.

Chemistry-consistent generative simulator.

To probe trimming behavior under controlled uncertainty, we use a minimal chemistry-consistent simulator as a development-time stress harness rather than as a surrogate for any full sequencing workflow. The simulator generates FASTQ-level reads by explicitly concatenating (i) a post-bisulfite genomic background segment with (ii) a chemistry-typed artifactual prefix, governed by a latent contamination-length random variable. This construction exposes per-read latent boundaries as ground truth even when exact boundary localization is intrinsically ill-posed in observational ssWGBS data, and avoids circular reliance on alignment- or methylation-level proxies for FASTQ-stage decisions.

Crucially, the simulator deliberately decouples the chemistry-typed baseline compositions from contamination-length structure, allowing structured regime shifts (including out-of-distribution length families and CpG-motivated stress) to be applied as independent perturbations. Accordingly, simulation results are interpreted as behavioral sanity checks and robustness stress tests of evidence accumulation, abstention, and stabilization logic, not as empirical performance claims on real datasets (Supplementary Note 7).

Practical baselines and reference points

Practice-driven reference points (fixed-length trimming).

In current ssWGBS preprocessing, removal of post-bisulfite enzymatic additions is most commonly implemented as a user-specified fixed cut length, often guided by vendor notes and pipeline defaults (e.g., a 10 bp heuristic is widely used in practice).[1, 2, 12, 13] Because a fixed cut is an operating choice rather than an identifiable FASTQ-stage quantity, it is routinely applied *without first establishing admissibility from FASTQ-level evidence* (i.e., without verifying that a chemistry-consistent artifact signature is present at the relevant read end; see more in Supplementary Note 1.2). Accordingly, fixed-length trimming serves as a pragmatic default but necessarily mixes over- and under-trimming when tail lengths are heterogeneous or long-tailed (Fig. 1C1), and we treat such settings as practice-driven reference points rather than as a canonical benchmark.

Development-time exploratory variants (context only).

During method development, we explored conservative variants to delineate which regions of the trimming decision space are supported by FASTQ-level evidence and which are intrinsically information-limited. These variants are mentioned only to clarify the Read 2 versus Read 1 feasibility asymmetry and to motivate the conservative design choices adopted in Y-Trim; they are not used for primary conclusions.

Reporting summaries for over- versus under-trimming

Because per-read ground-truth boundaries are not observable in real ssWGBS data without circularity, we avoid treating scalar “retention” or nominal “yield” as universal objectives: retained bases can reflect preserved genomic sequence or preserved synthetic carryover. Instead, we summarize trimming behavior along two chemistry-consistent directions that correspond to the two structural error modes of any boundary decision: (i) *avoidable genomic loss* due to over-trimming (cutting past the transition), and (ii) *residual artifact carryover* due to under-trimming (cutting before the transition). These summaries are computed in a short post-cut window using chemistry-typed background references and are used for reporting and visualization (not for optimizing the method); definitions and implementation details are in Supplementary Notes 7–8.

To connect preprocessing decisions to a methylation-relevant endpoint without requiring biological labels, we also report an *end-proximal* (early-position-weighted) excess-signal aggregation that emphasizes the region where boundary ambiguity and downstream sensitivity are both maximal (Supplementary Note 7).

Y-Trim framework

Scope and inputs.

Y-Trim is a pre-alignment, FASTQ-level preprocessing step applied after generic hygiene (e.g., adapter removal and coarse filtering). It uses only nucleotide identities (A/C/G/T/N) and positional order within a fixed read-start horizon, and does not use base-quality scores, alignment, read merging, or reference-genome context. An overview of the full decision flow is shown in Fig. 2.

Feasibility before inference.

Y-Trim separates (i) *admission control* (whether trimming is warranted at a given read end) from (ii) *boundary selection* (how far to trim when warranted). Admission control is implemented as a conservative, non-intervention principle: if chemistry-consistent evidence is not established at the sample level, trimming is not activated and the method returns *no action* (abstention) for that read end (Fig. 2 left-side admission branch).

Paired-end asymmetry.

Y-Trim treats paired-end reads asymmetrically, reflecting distinct physical origins of contamination. Read 2 is the primary inference target because tail-derived sequence is expected at its start under post-bisulfite geometry. When Read 2 is admitted at the sample level, its branch proceeds to texture-based evidence accumulation and conservative stopping (Fig. 2 R2 branch). Read 1 contamination arises only conditionally under read-through; accordingly, Y-Trim avoids per-read boundary localization for Read 1 and instead applies sample-level anchoring when Read 1 intervention is warranted (Fig. 2 R1 branch).

Sample-level admission control (gating)

Terminology (two levels of abstention).

Throughout, *abstention* denotes an explicit non-intervention outcome under FASTQ-level evidence constraints. In this work, abstention occurs at two distinct levels: (i) *sample-level abstention* from gating (do not activate trimming analysis for a read end), and (ii) *read-level abstention* after activation (return a zero cut for individual reads when read-level evidence is insufficient or unstable). These outcomes serve different roles and should not be conflated (Supplementary Note 2 for gating semantics; see Supplementary Notes 3–4 and 9 for Read 2 read-level behavior).

Role and inputs.

Gating determines *admissibility* of trimming analysis at a read end and returns a discrete outcome (*activate* vs. *abstain*); it does not perform boundary inference and does not determine cut positions. Operationally, gating implements a conservative non-intervention principle: if chemistry-consistent evidence is weak, inconsistent, or plausibly explained only by aggregation effects, trimming analysis is not activated for that read end (Fig. 2, left admission branch; cf. Fig. 1B and Supplementary Note 2).

All gating signals are computed from per-base sequence content (PBSC) over a fixed read-start window. Let $p_b(i)$ denote the PBSC at position i for base $b \in \{A, C, G, T\}$,

$$p_b(i) = \frac{1}{N} \sum_{r=1}^N \mathbb{I}[x_r(i) = b], \quad (1)$$

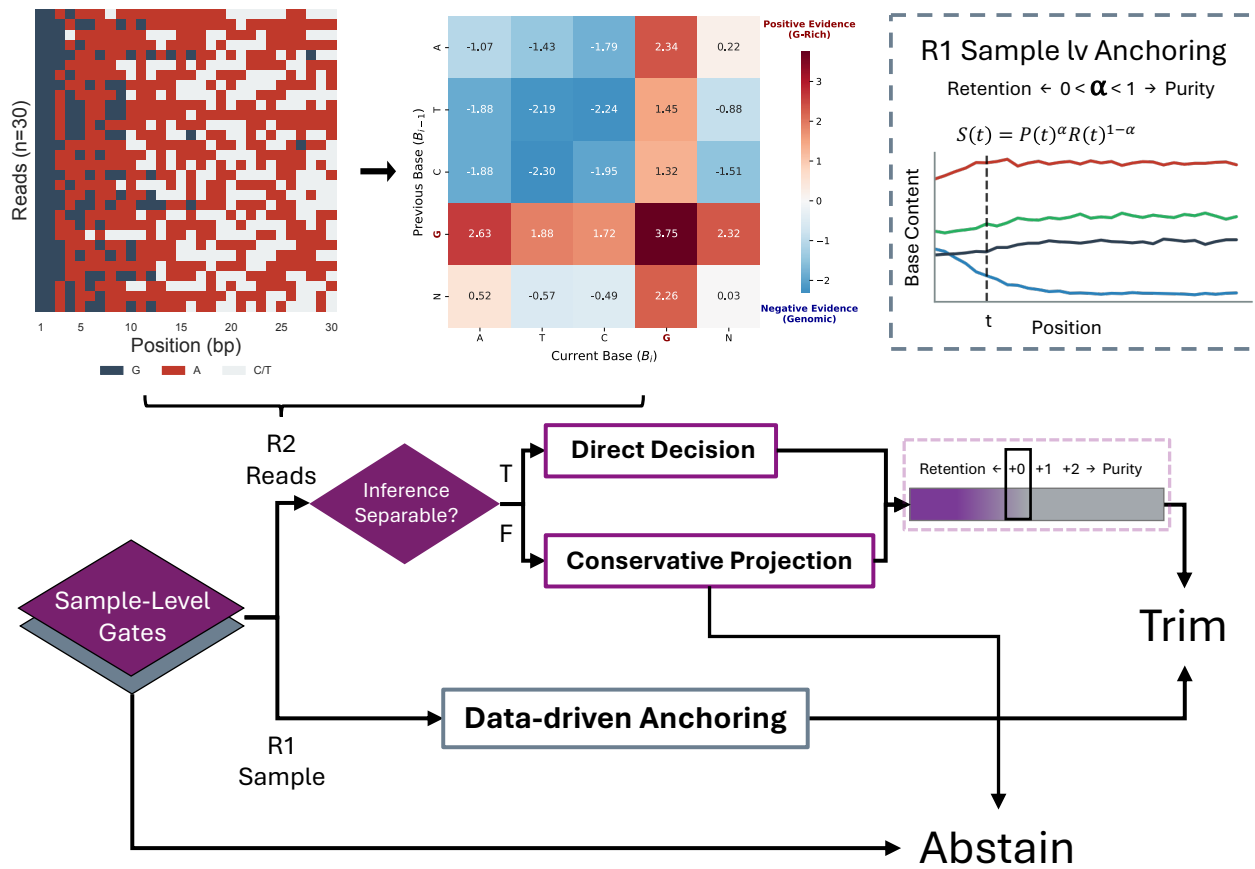


Figure 2 Y-Trim: evidence-gated trimming with explicit abstention and stabilization. Y-Trim decomposes trimming into (i) *admission control* (sample-level gating) that activates read-level action only when chemistry-consistent evidence is present, and (ii) *boundary selection* performed only on admitted reads. Read 2 is handled by deterministic texture-based evidence accumulation and conservative stopping, with a small integer offset selecting a deployment operating point on a fixed trade-off geometry. Read 1 is treated as a feasibility-limited regime and handled via sample-level anchoring rather than per-read boundary localization. A dedicated stabilization pathway handles long-tail inference breakdown without escalating aggressiveness, preserving bounded deployment behavior under heterogeneous contamination.

where $x_r(i)$ is the base observed at position i of read r (with \mathbb{N} treated as missing for PBSC).

Read 2 admission: ordered heterogeneous crossovers anchored at guanine.

For Adaptase-type ssWGBS, Read 2 commonly exhibits an early guanine-enriched synthetic regime with a transition toward bisulfite-converted genomic composition. We summarize this kinetic admissibility through the *ordering of the first crossover events* originating from guanine within a fixed inspection window. For bases $B_1, B_2 \in \{A, C, G, T\}$, define the first crossover position

$$\text{pos}(B_1 \rightarrow B_2) = \min \{i \leq L_{\text{cross}} : p_{B_2}(i) \geq p_{B_1}(i)\}, \quad (2)$$

with $\text{pos} = \infty$ if no crossover occurs in the window. Read 2 is admitted only when an *ordered* set of heterogeneous crossovers is observed: the first $G \rightarrow X$ crossover occurs early and the earliest such event is $G \rightarrow A$, accompanied by at least one additional heterogeneous crossover (e.g., $G \rightarrow C$ or $G \rightarrow T$), while later oscillatory intersections are intentionally ignored as unstable evidence (Supplementary Note 2.3).

Read 1 feasibility admission: geometry-limited lift under aggregation.

Read 1 artifacts arise conditionally via read-through ($L_{\text{read}} > L_{\text{insert}}$) and are not synchronized across reads, so admission is formulated strictly as a *sample-level feasibility check* rather than point estimation. We use a relative cytosine lift in the early prefix against an internal baseline window,

$$\Delta_C^{(R1)} = \frac{1}{|P|} \sum_{i \in P} p_C(i) - \frac{1}{|L|} \sum_{i \in L} p_C(i), \quad (3)$$

where P is a short early-prefix set and L is a later reference set within the read-start horizon. As a severe-case shortcut, the existence of an early crossover involving cytosine is also checked to rapidly identify strong read-through regimes with minimal assumptions; when present, this serves as a *fast-pass* to Read 1 feasibility admission rather than a boundary cue (Supplementary Note 2.4). Read 1 is admitted only when feasibility evidence is stable under aggregation and not dominated by short-scale fluctuations.

Semantics.

A gating outcome of *abstain* should be interpreted as *inadmissibility under FASTQ-level observables*, not as a claim that the sample is “clean” or free of artifacts. It indicates only that available sample-level evidence does not justify irreversible trimming at that read end (Supplementary Note 2.1–2.2).

Chemistry dependence and robustness.

Because PBSC near read starts varies with library chemistry and genomic background (e.g., across kits, protocols, and species), Y-Trim avoids absolute PBSC targets and instead uses relative, chemistry-consistent structure with conservative fallbacks so that changing the kit or the underlying genome does not break admission behavior (without retuning magnitude thresholds). The intended chemistry scope and robustness considerations are summarized in Supplementary Note 2.5–2.6.

Read 2 module: deterministic evidence accumulation and debounded stopping

Read 2 (R2) carries the direct kinetic footprint of Adaptase-mediated tailing and is the primary target for per-read boundary inference after sample-level admission is satisfied (Fig. 2, R2 branch; Supplementary Note 3). Inference operates exclusively on observed nucleotide identities from FASTQ (A/C/G/T/N) and positional order; no alignment, merging, or quality-score signals are used. We do not claim unique per-read boundary recovery; we claim bounded action under admissible evidence.

Evidence accumulation (matrix-linear trace).

For a read with bases $\{b_0, \dots, b_{L-1}\} \subset \Sigma$ where $\Sigma = \{A, C, G, T, N\}$, Y-Trim constructs a cumulative evidence trace over prefix length p within a fixed inference horizon L_{\max} :

$$S(p) = \beta_0 + \sum_{i=1}^p \mathbf{M}[b_{i-1}, b_i] + \mathbf{h}^\top \mathbf{c}_p + w_{\text{pos}} p, \quad 1 \leq p \leq L_{\max}. \quad (4)$$

Here $\mathbf{M} \in \mathbb{R}^{5 \times 5}$ is a fixed transition-score matrix, $\mathbf{c}_p \in \mathbb{R}^5$ is the prefix cumulative base-count vector, $\mathbf{h} \in \mathbb{R}^5$ is a fixed history-weight vector, and β_0, w_{pos} are fixed stabilizing terms. The transition term encodes short-range kinetic *texture* (Fig. 2, top-center heatmap), while the history and weak positional terms regularize behavior under low-contrast prefixes (Supplementary Note 3.1–3.2).

Stopping rule (debounced crossing).

A cut is produced only when the evidence trace indicates sustained departure from the synthetic-dominated regime. Define the run-length counter

$$k(p) = \begin{cases} k(p-1) + 1, & S(p) \geq 0, \\ 0, & S(p) < 0, \end{cases} \quad k(0) = 0.$$

Given a patience parameter $\pi \geq 0$, the inferred cut is

$$\hat{\ell} = \min\{p \in [1, L_{\max}] : k(p) \geq \pi + 1\}. \quad (5)$$

This “debounced” rule suppresses transient fluctuations: $\pi = 0$ is first-crossing; $\pi = 1$ requires two consecutive non-negative positions (Supplementary Note 3.3).

Per-read abstention and hard horizon.

If no $p \leq L_{\max}$ satisfies Eq. (5), the R2 solver *abstains* and returns “no deterministic placement” for this read, which triggers the conservative projection described next. This is a first-class information-limited outcome, not an algorithmic error (Supplementary Note 3–4). All R2 inference is constrained to a hard horizon $L_{\max} = 25$ bases; this bound is *not* an estimate of true tail length, but an epistemic truncation that bounds epistemic commitment once discriminative information becomes non-separating (Supplementary Note 3.1).

Conservative projection under R2 inference breakdown

When deterministic R2 inference fails to produce a confident stopping decision within L_{\max} (i.e., no deterministic stopping decision within L_{\max} ; Eq. (5)), Y-Trim applies a *post-inference conservative projection* that acts only on the already-computed cumulative evidence trajectory and introduces no new evidence (Fig. 2, R2 lower branch; Supplementary Note 4). Projection is an operational safeguard: it does not recover confidence or claim boundary correctness, but prevents arbitrary or overly aggressive trimming in entropy-dominated regimes.

Y-Trim implements two projection modes: a conservative composite default (**smart**) and a fully geometric alternative (**elbow**). Operational definitions and edge-case handling are provided in Supplementary Note 4.3.

Read 1 module: sample-level data-driven anchoring (purity–retention trade-off)

Read 1 (R1) contamination in ssWGBS arises conditionally through geometry-driven read-through rather than a localized enzymatic transition. As a result, per-read boundary inference for R1 is ill-posed on average and observable signals become coherent primarily under aggregation. Accordingly, Y-Trim handles R1 via a *sample-level anchoring* decision: it outputs a single trimming constant per sample (Fig. 2, R1 branch; Supplementary Note 5).

Anchoring objective and bounded search.

Anchoring resolves an interpretable trade-off between *purity* (suppression of residual synthetic signal) and *retention* (preservation of usable genomic sequence) under information limits, without claiming per-read boundary recovery (Supplementary Note 5.1). Candidate trim lengths are evaluated within a bounded search space at the R1 read end (3' end in read coordinates), restricted to ≤ 25 bases for stability (Supplementary Note 5.2).

Baseline-referenced scoring.

For each candidate trim length t , purity and retention are computed as baseline-referenced, sample-level summaries and normalized across the candidate set to avoid scale dependence. The anchored constant is chosen by maximizing a combined utility score of the form

$$S(t) = P(t)^\alpha R(t)^{1-\alpha}, \quad (6)$$

with a fixed $\alpha = 0.5$ (not tuned per sample) and practical safeguards (e.g., masking very small trim lengths) applied for robustness (Supplementary Note 5.3–5.5).

Deployment controls (offset vs. α).

Y-Trim exposes two conceptually different controls (Fig. 2, top-right inset). For Read 1 anchoring, α parameterizes the *purity–retention*

trade-off in the sample-level objective $S(t) = P(t)^\alpha R(t)^{1-\alpha}$. Because α changes the meaning of the objective itself, we treat it as a *method-level* setting and do not recommend modifying it without a clear deployment interpretation (Supplementary Note 5; implementation details in Supplementary Note 6.4).

For Read 2, a small discrete offset $o \in \{0, 1, 2\}$ is the *recommended* deployment knob: it selects an operating point on a fixed retained-genome versus residual-artifact trade-off *without changing the inference rule or evidence evaluation* (Supplementary Note 6.4).

Software implementation and reproducibility

Reference implementation.

Y-Trim is released as a transparent Python reference implementation intended to make the decision logic easy to inspect, run, and integrate. It is not positioned as an end-to-end preprocessing suite; instead, it serves as a minimal FASTQ-level transformer that can be incorporated into existing public or private pipelines wherever a paired-end FASTQ artifact-facing end is defined (Supplementary Note 6.1).

Deterministic behavior.

For a specified chemistry, all rules and parameters are fixed at deployment: no training, fitting, or dataset-adaptive estimation is performed at runtime. Chemistry-specific preparation (e.g., construction of fixed scoring components) is performed offline and amortized, leaving runtime behavior deterministic and reproducible (Supplementary Notes 6.5).

User-facing controls and supported scope.

Deployment controls are deliberately limited: α parameterizes the Read 1 purity-retention trade-off in the sample-level anchoring objective (method-level setting), whereas the Read 2 offset selects an operating point *without changing* evidence evaluation or stopping logic. Supported pipeline positioning, I/O semantics, and practical integration guidance (including what is and is not validated) are documented in Supplementary Note 6.6.

Results

CCGB-34 reveals asymmetric decision geometry between Read 2 and Read 1

We evaluated Y-Trim on CCGB-34 using the common reporting axes defined in Supplementary Note 8.2.3–8.2.4, restricting summaries to samples that passed admission for the relevant read end (i.e., where trimming was deemed admissible under PBSC-level evidence). This avoids conflating deployment behavior with samples for which Y-Trim correctly returns no action.

Read 2 forms a navigable frontier.

On Read 2, admitted samples exhibit a coherent trade-off geometry between residual synthetic signal and retained genomic bases (Fig. 3A1). Varying the deployment offset traverses this frontier in an interpretable way: offset selects operating points along a fixed decision geometry *without changing* the underlying evidence accumulation and stopping rule. A fixed 10 bp trim falls in the same general region of the frontier, consistent with its role as a pragmatic engineering fallback when Read 2 tailing is systematic, but it does

not provide admission semantics and cannot adapt to long-tailed heterogeneity.

Read 1 collapses into a feasibility-limited cluster, and naive fixed trimming can be catastrophic.

In contrast, Read 1 does not yield a meaningful frontier (Fig. 3A2). Adaptive attempts concentrate into an unstructured cluster consistent with geometry-limited feasibility: contamination arises conditionally through read-through and is not synchronized across reads, so per-read boundary navigation is not supported even when aggregate effects are visible. Importantly, the effective axis range in A2 is markedly different from A1: the naive fixed 10 bp trim becomes an extreme outlier that achieves low residual artifact only by incurring severe avoidable genomic loss (retention collapse), illustrating why treating Read 1 as a “weaker Read 2” is a category error in post-bisulfite libraries.

Practical overhead.

These gains in decision interpretability do not rely on heavy downstream signals: in the supported pre-merge setting, Read 1 uses a one-time sample-level pass for anchoring, while Read 2 operates on a fixed short prefix per read, yielding predictable preprocessing cost. Reference-implementation timings are reported for transparency in Supplementary Note 8.3 and should be interpreted as practical sanity checks rather than performance claims.

Simulator-backed OOD stress isolates behavior under controlled regime shift

Because per-read ground-truth boundaries are not observable in real ssWGBS data without circularity, we use a minimal chemistry-consistent simulator to probe *behavior under controlled uncertainty* (Supplementary Note 7.2). The simulator provides explicit latent boundaries while deliberately decoupling chemistry-typed baseline composition from contamination-length structure, enabling stress tests that vary tail-length families and regime structure without changing the deployed decision rule.

Across out-of-distribution (OOD) contamination-length families, Y-Trim remains stable and chemistry-consistent under fixed parameters (Fig. 3B). Crucially, the decision rule is held constant—including the R2 evidence trace, debounced stopping, and hard horizon—while only the latent length structure is perturbed. Under these regime shifts, the resulting trimming behavior changes in a structured way: outputs preserve the ordering and qualitative separation induced by the imposed length families, rather than collapsing to a single default cut or exhibiting unstructured drift. This pattern is consistent with a texture-driven interface that responds to admissible FASTQ-level evidence, not with a rule that encodes a single implicit tail-length prior.

These checks do not aim to certify physical boundary recovery; they validate that the deployed FASTQ-level decision interface responds coherently to controlled regime shifts in the only latent factor we perturb (tail-length structure), under otherwise fixed chemistry-typed observables.

End-proximal, CpG-sensitive aggregation makes operating-point trade-offs explicit

In methylation contexts, the most consequential uncertainty is concentrated near read ends: small end-proximal artifacts

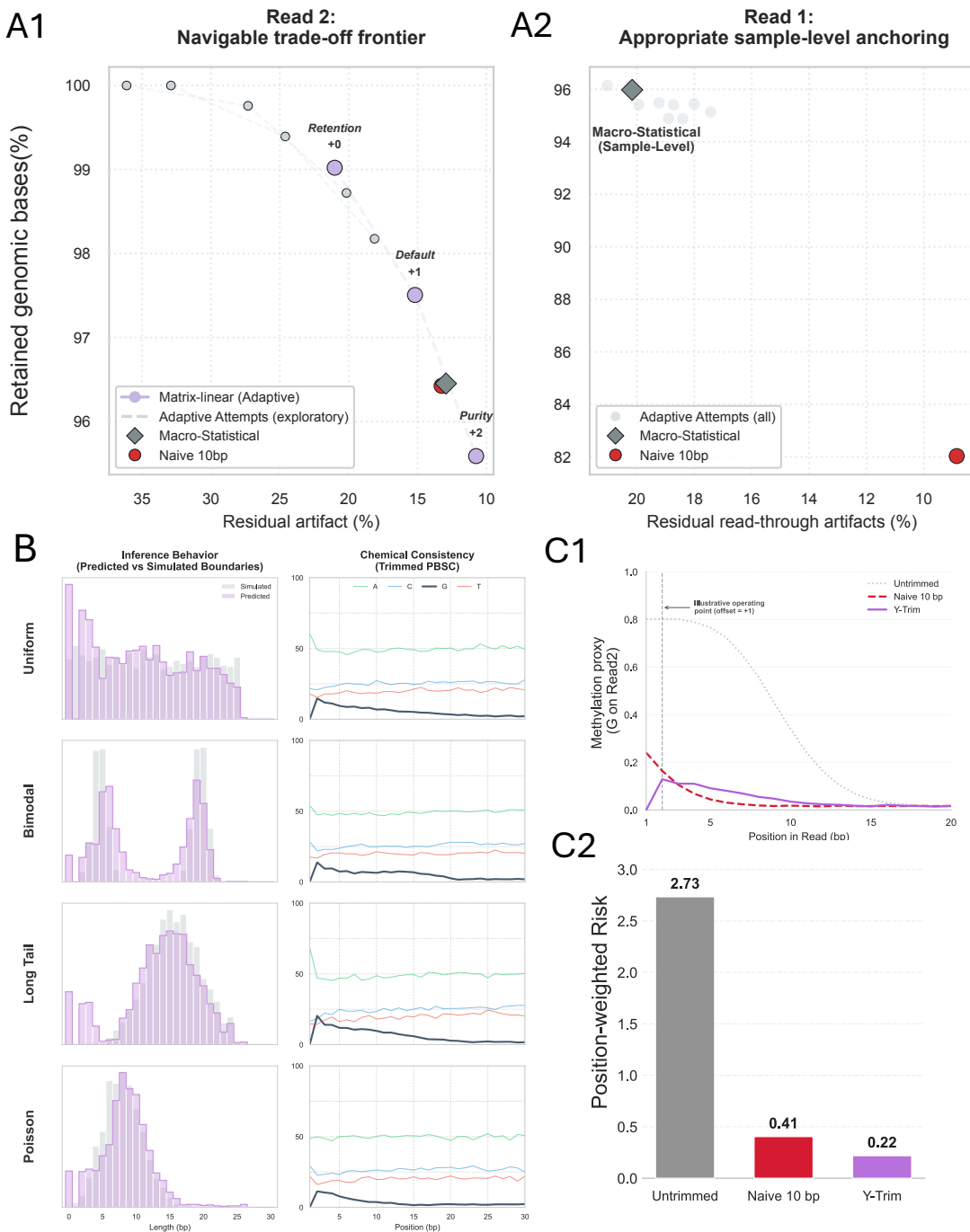


Figure 3 Asymmetric decision geometry and robustness under regime shift and CpG-sensitive stress. (A1) On CCGB-34 Read 2, adaptive trimming exposes a navigable frontier between residual synthetic signal and retained genomic bases; offset selects interpretable operating points along a fixed decision geometry without changing inference. (A2) On Read 1, adaptive attempts collapse into an unstructured cluster consistent with geometry-limited feasibility, motivating conservative sample-level anchoring and abstention rather than read-level frontier navigation. (B) Simulator-backed out-of-distribution (OOD) stress tests: across diverse contamination-length families, Y-Trim remains stable and chemistry-consistent under fixed decision rules, indicating robustness to regime shift rather than reliance on a single tail-length prior. (C) CpG-motivated stress evaluation emphasizes early-position sensitivity in methylation contexts: (C1) post-trim Read 2 dominant-G signal is suppressed in a way that avoids false-positive “cleanliness” artifacts driven by local texture fluctuations, and (C2) an end-proximal, position-weighted excess-signal score compares Y-Trim operating points against a commonly used fixed-length reference (10 bp) under CpG-sensitive risk aggregation.

can propagate nonlinearly into methylation-relevant summaries, especially for fragmented or low-input DNA where usable evidence is already concentrated near read starts/ends. In Adaptase-based post-bisulfite ssWGBS, the dominant-*G* structure at the Read 2 start is precisely the kind of artifact that can create *false end cleanliness* or *false end signal* under downstream aggregations that overweight early positions (e.g., CpG-end-sensitive summaries). We therefore treat post-trim Read 2 dominant-*G* excess as an end-proximal risk proxy: it is directly observable at the FASTQ stage, it targets the region where downstream sensitivity is maximal, and suppressing it reduces the opportunity for early-position synthetic structure to masquerade as usable methylation-relevant sequence. Guanine also serves as the most robust chemistry-consistent discriminator for Adaptase tailing in the regimes studied here, providing a stable anchor for both admission and post-hoc reporting. We summarize outcomes using an end-proximal, position-weighted excess-signal aggregation that emphasizes this high-leverage region (Supplementary Note 7.3).

C1: Content-aware suppression versus fixed translation.

Fig. 3C1 shows how Read 2 dominant-*G* signal returns toward a chemistry-consistent post-bisulfite baseline after trimming. A fixed-length trim (e.g., 10 bp) acts as a *content-agnostic translation*: it effectively shifts the pre-trim profile inward by a constant, without interrogating whether residual artifact-like sequence remains beyond that point (cf. the fixed-cut mismatch in Fig. 1C2). In contrast, Y-Trim's Read 2 rule is *content-aware*: it accumulates local texture evidence and stops only when sustained departure from the synthetic-dominated regime is supported. Operationally, this behaves as a targeted “search-and-destroy” of end-proximal false-positive artifact signal, producing a suppressed near-zero start followed by a smooth relaxation toward the genomic background rather than a rigidly translated curve. While any single base position can favor one heuristic under heterogeneity, the most fragile early region is the primary target of conservative trimming behavior.

C2: End-proximal aggregation as a risk-emphasis lens.

To make this early-region behavior comparable in a single summary, we use an end-proximal, position-weighted excess-signal score (Fig. 3C2; Supplementary Note 7.3). The weighting is not claimed to be uniquely optimal; it is a conservative *risk-emphasis* choice that increases sensitivity to end-localized spikes, since concentrated residual signal near the read start is more likely to manifest as systematic false-positive “cleanliness” or localized bias than diffuse low-amplitude drift. Under this aggregation, Y-Trim's recommended offsets are competitive with a commonly used fixed-length reference (10 bp), while making explicit the purity–retention trade-off implied by any irreversible trimming decision. The fixed-length reference is used only as a practice-driven coordinate for comparison, not as a FASTQ-stage quantity with a uniquely correct interpretation.

Discussion

Trimming in post-bisulfite ssWGBS is often treated as a generic preprocessing knob, but our results emphasize that it is fundamentally a *FASTQ-stage* decision problem: the only universally admissible evidence is the observed base string and its position. Under bisulfite-induced compositional collapse, genomic and synthetic origins can share support under the same observable alphabet, creating an intrinsically indistinguishable transition regime and a

non-zero error floor for any deterministic per-read point estimate (Supplementary Note 1). This shifts the appropriate objective away from “exact” boundary recovery and toward *bounded, chemistry-consistent risk control* under explicit uncertainty.

Taking the data-generating asymmetry seriously explains the qualitative structure seen in CCGB-34. Read 2 carries systematic Adaptase-derived signal at the read start, so admitted samples exhibit a coherent, navigable decision geometry: deployment offset traverses an interpretable frontier between residual artifact-like signal and retained genome-like bases without changing inference logic (Fig. 3A1; Supplementary Notes 2 and 3). Read 1 behaves differently: contamination is conditional on insert-length geometry and becomes coherent primarily under aggregation, so read-level adaptivity collapses into an unstructured cluster rather than a frontier (Fig. 3A2). This is not a weaker version of Read 2, but a different inferential regime; treating it as “weaker R2” is precisely what produces the pathological behavior of fixed-length trimming in Read 1.

These constraints motivate a staged design in which *feasibility is assessed before inference* and irreversible action is taken only under admissible evidence. In Y-Trim, sample-level admission (gating) serves as a non-intervention principle, preventing trimming when PBSC structure is weak, inconsistent, or plausibly explained only by aggregation effects (Supplementary Note 2). After admission, Read 2 uses deterministic evidence accumulation with debounced stopping and an explicit hard horizon to avoid false precision once marginal information collapses (Supplementary Note 3). When inference exhausts, uncertainty is handled as a first-class outcome via post-inference conservative projection rather than escalating aggressiveness (Supplementary Note 4). Read 1 is handled by sample-level anchoring that resolves a purity–retention trade-off under geometry-limited uncertainty without claiming per-read boundary localization (Supplementary Note 5).

A practical implication is that deployment should make the remaining degrees of freedom explicit. Offset is a recommended operating-point selector that moves along an existing Read 2 decision geometry *without* changing evidence evaluation, whereas α changes the meaning of the Read 1 anchoring objective itself and is therefore not a routine tuning knob (Supplementary Note 6). More broadly, the evidence-gated framing is not specific to ssWGBS: it applies to other template-free, texture-defined end artifacts where the synthetic process shares the same observable alphabet as biological sequence. The transfer requirement is not a shared motif but a chemistry-consistent, locally observable statistical signature and a validation path (e.g., simulator-backed stress) that prevents over-claiming in information-limited regimes (Supplementary Note 7).

Conclusion

Single-stranded bisulfite sequencing enables methylation profiling in low-input and fragmented samples, but post-bisulfite library construction introduces stochastic end artifacts that limit what can be inferred about read boundaries from FASTQ observables alone. Because synthetic and genomic sequence share support under the same nucleotide alphabet, a non-zero error floor is unavoidable in an indistinguishable transition regime (Supplementary Note 1), making per-read “exact” boundary recovery ill-posed for a subset of reads. This structure explains both why fixed-length trimming persists as

a pragmatic default and why it is systematically mismatched to heterogeneous, long-tailed tailing behavior.

We provide three contributions. (1) We formalize ssWGBS trimming as a constrained, asymmetric decision problem and introduce Y-Trim, a white-box framework that separates feasibility from inference, handles Read 2 and Read 1 according to their distinct physical origins, and exposes interpretable operating points for conservative deployment. (2) We construct a chemistry-consistent simulator with per-read ground truth alongside a curated real-data collection (CCGB-34), enabling controlled evaluation of inference behavior without relying on unobservable boundary labels in real data. (3) We show that making trimming decisions explicit yields an interpretable genomic-retention versus residual-artifact frontier on CCGB-34 and reduces end-proximal artifactual signal in methylation-relevant summaries, supporting uncertainty-aware preprocessing in ssWGBS.

Conflicts of interest

The authors declare that they have no competing interests.

Funding

This work was conducted without external grant funding. Publication-related costs are supported through institutional open access resources.

Data Availability

All sequencing datasets analyzed in this study are publicly available from NCBI repositories (GEO/SRA/BioProject). The CCGB-34 cohort (Comprehensive Cell-free & Genomic Bisulfite; $n = 34$) was assembled from seven published studies and associated accessions: GSE178666/SRP325062 [5], GSE307705/SRP619043 [6], SRP299418 [7], GSE249140/SRP475142 [8], PRJNA1162448/SRP533334 [9], PRJNA1348139/SRP636882 [10], and PRJNA1328772/SRP620537 [11]. No new sequencing data were generated for this study.

A complete reference implementation of Y-Trim (core inference engine, simulator, demo, and full figure-reproduction workflows) is available for peer review via a view-only OSF link: https://osf.io/etqrj/overview?view_only=795c81dbfa8a4f7185b1c45310628591. The package includes scripts to reproduce all analyses and figures reported in the manuscript. Upon acceptance, the code will be released publicly under the MIT License, and an archived release will be deposited in a long-term repository (e.g., Zenodo or OSF).

Supplementary Data

Supplementary Data are available at *NAR* Online.

Acknowledgements

We are deeply grateful to Prof. Lenore Cowen for sustained mentorship, critical guidance on research direction and positioning, and extensive feedback throughout the development of this work. We are grateful to Dr. Yongkun Ji for discussions that clarified the ssWGBS chemistry and pipeline context, and for feedback that improved domain framing and technical conventions. We thank Dr.

Rebecca Batorsky for detailed feedback on validation strategy and presentation, and for emphasizing the importance of evaluating downstream biological consequences during method development. We thank Jindan Huang for valuable advice on research planning and publication strategy. We thank Dr. William White for helpful discussions, broader scientific feedback, and advice on manuscript presentation. We thank Prof. Jivko Sinapov for early developmental discussions and algorithmic perspective. We also thank Dr. Albert Tai for technical discussions regarding sequencing workflows, as well as Hiu Mai and Yijia Zhang for preliminary literature exploration.

Author Contributions

Y.F. conceived the project, developed the theoretical framework and algorithms, performed all computational analyses, and wrote the manuscript.

References

1. Swift Biosciences. Accel-NGS 1S Plus and Methyl-Seq: Tail Trimming for Better Data. Technical Note, Swift Biosciences, 2015. Available at: <https://www.genetargetsolutions.com.au/wp-content/uploads/2015/05/Accel-NGS%2C2%AE-1S-Plus-Methyl-Seq-Tail-Trimming-For-Better-Data-1.pdf>.
2. Swift Biosciences. Tail Trimming for Better Data: Accel-NGS Methyl-Seq, Adaptase Module and 1S Plus DNA Library Kits. Technical Note, Swift Biosciences, 2019. Available at: <https://www.biocience.co.uk/userfiles/pdf/16-0853-Tail-Trim-Final-442019.pdf> (accessed 2026-01-30).
3. Fumihiro Miura, Yusuke Enomoto, Ryo Dairiki, and Takashi Ito. Amplification-free whole-genome bisulfite sequencing by post-bisulfite adaptor tagging. *Nucleic Acids Research*, 40(17):e136, 2012. doi: <https://doi.org/10.1093/nar/gks454>.
4. Fumihiro Miura, Yukiko Shibata, Miki Miura, Yuhei Sangatsuda, Osamu Hisano, Hiromitsu Araki, and Takashi Ito. Highly efficient single-stranded DNA ligation technique improves low-input whole-genome bisulfite sequencing by post-bisulfite adaptor tagging. *Nucleic Acids Research*, 47(15):e85, 2019. doi: <https://doi.org/10.1093/nar/gkz435>.
5. Jia Li, Y. Huang, and X. Li. Cerebrospinal fluid cell-free DNA methylomes recapture pediatric medulloblastoma tissue's tumor feature. NCBI GEO, 2024. Accession: GSE178666 / SRP325062. <https://www.ncbi.nlm.nih.gov/geo/query/acc.cgi?acc=GSE178666>.
6. Christa Caggiano, Marco Morselli, Xiaoyu Qian, Barbara Celona, Michael J. Thompson, Shivangi Wani, et al. Epigenetic profiles of tissue informative CpGs inform ALS disease status and progression. *Genome Medicine*, 17(1):115, 2025. doi: <https://doi.org/10.1186/s13073-025-01542-5>. Data: GSE307705 / SRP619043.
7. Alexandre P. Cheng, Sean Donnelly, Kayla Queen, Chaggai Ukaegbu, et al. Cell-free DNA profiling of critically ill COVID-19 patients reveals tissue damage and virus footprints. *Cell Reports Medicine*, 2(10):100428, 2021. doi: <https://doi.org/10.1016/j.xcrm.2021.100428>. Data: SRP299418.

8. Emily K. W. Lo, A. Idrizi, R. Tryggvadottir, W. Zhou, Andrew P. Feinberg, et al. DNA methylation memory of pancreatic acinar-ductal metaplasia transition state altering Kras-downstream PI3K and Rho GTPase signaling in the absence of Kras mutation. *Genome Medicine*, 17(1):32, 2025. doi: <https://doi.org/10.1186/s13073-025-01542-6>. Data: GSE249140 / SRP475142.
9. Children's Mercy Research Institute. Methylation patterns of the nasal epigenome of hospitalized SARS-CoV-2 positive patients reveal insights into molecular mechanisms of COVID-19. NCBI BioProject, 2024. Accession: PRJNA1162448 / SRP533334. <https://www.ncbi.nlm.nih.gov/bioproject/PRJNA1162448>.
10. University of Heidelberg. Chamber-Specific Chromatin Architecture Guides Functional Interpretation of Disease-Associated Cis-Regulatory Elements in Human Cardiomyocytes. NCBI BioProject, 2025. Accession: PRJNA1348139 / SRP636882. <https://www.ncbi.nlm.nih.gov/bioproject/PRJNA1348139>.
11. Alvaro Quintanal-Villalonga, Hirokazu Taniguchi, Yingqian A. Zhan, Maysun M. Hasan, Shweta S. Chavan, Fanli Meng, et al. Multiomic Analysis of Lung Tumors Defines Pathways Activated in Neuroendocrine Transformation. *Cancer Discovery*, 11(12):3028–3047, 2021. doi: <https://doi.org/10.1158/2159-8290.CD-20-1863>. Data: PRJNA1328772 / SRP620537.
12. Marcel Martin. Cutadapt removes adapter sequences from high-throughput sequencing reads. *EMBnet.journal*, 17(1):10–12, 2011. doi: <https://doi.org/10.14806/ej.17.1.200>.
13. Felix Krueger, Frankie James, Phil Ewels, Ebrahim Afyounian, and Benjamin Schuster-Boeckler. Trim Galore! v0.6.7. Zenodo, 2021. doi: <https://doi.org/10.5281/zenodo.5127899> (accessed 2026-01-30).
14. Felix Krueger and Simon R. Andrews. Bismark: a flexible aligner and methylation caller for Bisulfite-Seq applications. *Bioinformatics*, 27(11):1571–1572, 2011. doi: <https://doi.org/10.1093/bioinformatics/btr167>.
15. Aimée M. Deaton and Adrian Bird. CpG islands and the regulation of transcription. *Genes & Development*, 25(10):1010–1022, 2011. doi: <https://doi.org/10.1101/gad.2037511>.
16. Zahava Siegfried and Itamar Simon. DNA methylation and gene expression. *WIREs Systems Biology and Medicine*, 2(3):362–371, 2010. doi: <https://doi.org/10.1002/wsbm.64>.
17. Huiyan Luo, Wei Wei, Ziyi Ye, Jiabo Zheng, and Rui-hua Xu. Liquid Biopsy of Methylation Biomarkers in Cell-Free DNA. *Trends in Molecular Medicine*, 27(5):482–500, 2021. doi: <https://doi.org/10.1016/j.molmed.2020.12.011>.
18. Hu Zeng, Bo He, Chengqi Yi, and Jinying Peng. Liquid biopsies: DNA methylation analyses in circulating cell-free DNA. *Journal of Genetics and Genomics*, 45:185–192, 2018. doi: <https://doi.org/10.1016/j.jgg.2018.02.007>.
19. Ryan Lister, Mattia Pelizzola, Robert H. Dowen, R. David Hawkins, Gary Hon, Julian Tonti-Filippini, Joseph R. Nery, Leonard Lee, Zhen Ye, Que-Minh Ngo, et al. Human DNA methylomes at base resolution show widespread epigenomic differences. *Nature*, 462(7271):315–322, 2009. doi: <https://doi.org/10.1038/nature08514>.